J. Fluid Mech. (2009), *vol.* 637, *pp.* 305–325. © Cambridge University Press 2009
doi:10.1017/S0022112009990504

Time-dependent response of a heterogeneous elastic plate floating on shallow water of variable depth

IZOLDA V. STUROVA†

Lavrentyev Institute of Hydrodynamics, Lavrentyev Prospect 15, 630090 Novosibirsk, Russia

(Received 12 August 2008; revised 18 May 2009; accepted 19 May 2009; first published online 18 September 2009)

The problem of unsteady behaviour of a floating thin plate is solved. The simultaneous motion of the plate and the fluid is considered within the framework of linear shallow-water theory. It is assumed that the bottom is not uniform in depth under the heterogeneous plate represented by an infinitely extended strip of finite width. The elastic deflection of the plate is expressed by a superposition of modal functions of a homogeneous beam with free edge conditions. The time-dependent unknown amplitudes are determined from the solution of a linear set of ordinary differential equations with constant coefficients. The eigenvalues of this set are determined numerically. Proposed method is used for the solution of three unsteady problems: the scattering of localized surface wave by an elastic plate, decay of the initial deformation of the plate in the fluid at rest and the action of a periodic load on a plate. Numerical calculations are performed for the ice sheet with the variable thickness and various bottom topographies.

1. Introduction

Unsteady forcing of a floating thin plate can be used to model a wide range of physical systems: for example, very large floating structures, sea ice floes and breakwaters. Because of their large size and small thickness, the elastic response of such structures is significant. At present, there exists an extensive literature on hydroelastic analysis of the floating platforms (see, for example, the reviews by Watanabe, Utsunomiya & Wang 2004; Ohmatsu 2005; Chen *et al.* 2006). The interactions of sea ice and ocean waves are considered in recent review by Squire (2007). Much attention in this review is given to effect of various irregularities in an ice sheet.

However, the effect of structure heterogeneity and a varying water depth was investigated only for diffraction problem, by solving the linear hydroelastic problem for a single frequency (see, for example, Porter & Porter 2004; Bennetts, Biggs & Porter 2007). The aim of this paper is to consider the unsteady hydroelasticity problem for a heterogeneous plate floating on shallow water of variable depth. This problem has been chosen because the sea-bottom effects become more significant in shallow water, than that in deep water. The actual floating structures (both the ice floes and the manufactured platforms) show variability on all spatial scales.

† Email address for correspondence: sturova@hydro.nsc.ru

https://doi.org/10.1017/S0022112009990504 Published online by Cambridge University Press

In contrast to the single-frequency solutions, solving time-dependent hydroelastic systems remains a difficult problem. Even for linear formulation the solution of three-dimensional transient problem for the finite floating plate is a complicated task that requires high computational cost. Only a limited number of studies on this kind of the problem have been reported to date. For example, Watanabe & Utsunomiya (1996) presented the numerical results of the elastic responses of a very large circular floating structure excited by impulsive loading. Meylan (1997) considered the periodic forced vibrations of an arbitrary thin plate floating on the surface of an infinitely deep fluid. Using a spectral method, he applied these results for the consideration of the time-dependent motion of the rectangular plate due to an impulsive forcing pressure. Ohmatsu (1998) proposed a calculation method based on Fourier transforms, adopting the frequency-domain response function to analyse the behaviour of a floating structure influenced by an arbitrary changing load. Endo & Yago (1999) carried out experiments under three loading conditions – weight drop test, weight pull-up test and weight moving test which idealize the airplane landing and take-off. They also developed a time-domain analysis method based on a finite element method (FEM) scheme, which utilized the memory effect function for hydrodynamic effects. Kashiwagi (2000, 2004) has developed a numerical method for the time-dependent elastic deflection of a structure by utilizing a superposition of mathematical modal functions. Lee & Choi (2003) proposed a hybrid method to analyse the transient hydroelastic response of a floating structure by utilizing boundary element method for fluid domain and FEM for plate domain. Qui & Liu (2005) developed a time-dependent FEM to analyse the transient hydroelastic responses of a floating structure subjected to dynamic loads. In most of the numerical methods, a floating structure is modelled as a simple rectangular or circular plate. The three-dimensional unsteady hydroelastic problem is simplified for an elastic plate floating on shallow water. Sturova (2003) considered the behaviour of a circular elastic plate under the action of an external load by using a superposition of modal functions.

There are some studies in which the two-dimensional unsteady hydroelastic problem is considered. In this case the elastic plate presents an infinitely extended elastic strip of finite width. It is assumed that the properties of the strip, the bottom and the unsteady load do not depend on the horizontal direction along the strip. The time-dependent behaviour of an elastic strip floating on shallow water has been investigated by Meylan (2002) and Sturova (2002*b*). Meylan (2002) used a spectral method for a massless elastic plate and considered the scattering of localized surface wave by an elastic plate and the behaviour of the plate caused by its initial deformation in the fluid at rest. Sturova (2002*b*) studied the behaviour of floating plate under external loading by using a mode-expansion method and a time-stepping procedure. The response of the plate under different impulsive and moving loadings with and without allowance for the inertia of load was considered. It was shown that in the general case of the motion of a massive load on the plate with large acceleration, the inertial forces arising due to combined oscillations of this load and the plate (inertial loading) should be taken into account.

Sturova (2006*b*) employed the mode-expansion method and the memory-effect functions to study the behaviour of a strip floating on the surface of an infinitely deep fluid. Unsteady response of an elastic strip subjected to initial perturbations and different external loadings was investigated. In the two-dimensional problem, it is possible to avoid the assumptions introduced for the three-dimensional problem in Endo & Yago (1999) and Kashiwagi (2000, 2004) to determine the memory functions

https://doi.org/10.1017/S0022112009990504 Published online by Cambridge University Press

because the behaviour of damping coefficients in the high-frequency limit is known exactly for the radiation problem.

Time-dependent behaviour of the elastic strip floating on water of finite depth was studied by Hazard & Meylan (2007) and Qui (2007). Hazard & Meylan (2007) presented two spectral theories based on the first-order and second-order formulations of the problem. The first-order theory is valid only for a massless plate, while the second-order theory applies for a plate with mass. As in Meylan (2002), the scattering of localized surface wave by an elastic plate and the behaviour of the plate caused by its initial deformation in the fluid at rest are considered. Qui (2007) developed a time-domain FEM to analyse the dynamic response of a floating plate under the effects of impulsive and moving loads. The results for a moving load were compared with the results by Sturova (2002*b*) and good agreement was observed. Significant effects of the travelling speed, the water depth and the width of a strip on the behaviour of floating elastic strip subjected to moving loads were shown. In all of these studies of unsteady hydroelastic problem, the floating structure was idealized as a homogeneous elastic plate and the fluid was assumed either infinitely deep or with a flat bed.

In this paper, a time-domain method is developed to analyse the hydroelastic response of a heterogeneous strip floating on shallow water of variable depth. The simultaneous motion of the plate and the fluid is considered within the framework of linear theory. This paper is the extension of two papers by Sturova (2008*a*, *b*). Effect of variable depth on time-dependent response of a homogeneous elastic plate is considered in the first paper. Unsteady behaviour of a heterogeneous plate floating on shallow water with a flat bed is studied in the second paper. Two methods were presented for the solution of this problem. Both the methods are based on the expansion of the plate motion in the dry modes of vibration of the free plate. The eigenfunctions of a heterogeneous plate were used in the first method, whereas the eigenfunctions of a homogeneous plate were used in the second method. A correlation between two methods was demonstrated for the elastic plate with piece-wise constant functions for the flexural rigidity and mass. It was shown a good quantitative agreement between the numerical results of these two methods. Unfortunately, free natural modes of vibration can only be determined analytically for very few heterogeneities, for example, if the flexural rigidity and mass of the elastic plate are piece-wise constant functions. More general heterogeneities demand a numerical approach. As a consequence, the use of the eigenfunctions of a homogeneous plate is more preferentially for the arbitrary heterogeneities. Three unsteady problems were considered in Sturova (2008*a*): the scattering of localized surface wave by an elastic plate, the behaviour of the plate caused by its initial deformation in the fluid at rest and the effect of a moving external load. Only the first two unsteady problems were studied in Sturova (2008*b*).

In this paper, the elastic deflections of the plate are expressed by a superposition of modal functions of a homogeneous beam with free edge conditions. Proposed method may be used for any unsteady two-dimensional problem of linear shallow-water theory, but here this method is used for three problems: the incidence of a localized surface wave on a plate, the initial deformation of a plate, and the action of a periodic load on a plate.

2. Mathematical formulation

Figure 1 shows a schematic diagram of the problem. An elastic heterogeneous plate floats on the surface of an inviscid incompressible fluid layer which is bounded below

https://doi.org/10.1017/S0022112009990504 Published online by Cambridge University Press

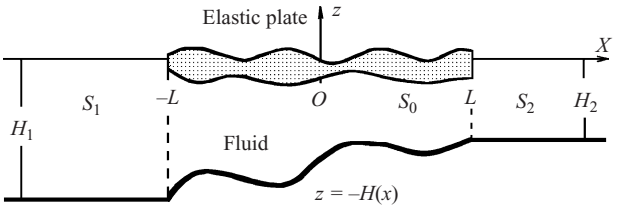


FIGURE 1. Schematic diagram of a heterogeneous plate floating on shallow water of variable depth.

by a fixed impermeable bed. The plate is infinite in the y direction, so that only the x and z directions are considered. The x direction is horizontal, the positive z-axis points vertically up, and the plate covers the region $-L \leqslant x \leqslant L$. The surface of the fluid that is not covered with the plate is free. The fluid region S is divided into three parts: S_0 ($|x| < L$), S_1 ($x < -L$) and S_2 ($x > L$). Without the plate, the fluid depth is equal to $H(x)$ in S_0, and the fluid depths in the left- and right-hand domains of constant depth S_1 and S_2 are equal to H_1 and H_2, respectively. With the plate, the fluid depth in S_0 is equal to $h(x) = H(x) - d(x)$, where $d(x)$ is the variable draft of the plate. It is assumed that the maximal depth of the fluid is small in comparison with the length of the surface and the flexural-gravity waves, and the shallow water approximation is used. The fluid flow is assumed to be irrotational. The velocity potentials describing the fluid motion in the regions S_j are denoted by $\phi_j(x, t)$ ($j = 0, 1, 2$), where t is time.

A deflection of a heterogeneous elastic plate $w(x, t)$ is described by the equation:

$$\frac{\partial^2}{\partial x^2}\left(D(x)\frac{\partial^2 w}{\partial x^2}\right) + m(x)\frac{\partial^2 w}{\partial t^2} + g\rho w + \rho\frac{\partial \phi_0}{\partial t} = -p(x, t), \quad (|x| \leqslant L), \tag{2.1}$$

where $D(x)$ is the flexural rigidity of the plate, $m(x)$ is the mass per unit length of the plate, ρ is the fluid density, g is the gravity acceleration and $p(x, t)$ denotes the external load acting upon the plate. According to Archimedes' principle,

$$\int_{-L}^{L} [m(x) - \rho d(x)]\, \mathrm{d}x = 0. \tag{2.2}$$

The functions $D(x)$ and $m(x)$ must have an integrable second derivatives, be piecewise continuous themselves, and must have piecewise continuous first derivatives. For the case of a homogeneous plate, we have the constant values for D, m and d (see, for example, Sturova 2002*b*).

According to linear shallow-water theory, the following relation is valid (Stoker 1957):

$$\frac{\partial w}{\partial t} = -\frac{\partial}{\partial x}\left(h(x)\frac{\partial \phi_0}{\partial x}\right), \quad (x \in S_0). \tag{2.3}$$

In the free-water regions, the velocity potentials $\phi_1(x, t)$ and $\phi_2(x, t)$ satisfy the equations

$$\frac{\partial^2 \phi_j}{\partial t^2} = g H_j \frac{\partial^2 \phi_j}{\partial x^2} \quad (x \in S_j), \quad (j = 1, 2). \tag{2.4}$$

Far from the plate, the wave motion goes to zero

$$\frac{\partial \phi_1}{\partial x} \to 0 \quad (x \to -\infty), \quad \frac{\partial \phi_2}{\partial x} \to 0 \quad (x \to \infty). \tag{2.5}$$

https://doi.org/10.1017/S0022112009990504 Published online by Cambridge University Press

The displacements of the free surface $\eta_1(x,t)$ and $\eta_2(x,t)$ are determined in the regions S_1 and S_2 from the relations

$$\eta_j = -\frac{1}{g}\frac{\partial \phi_j}{\partial t} \quad (x \in S_j), \quad (j = 1, 2). \tag{2.6}$$

If $|x| = L$, the matching conditions (continuity of pressure and mass) should be satisfied:

$$\frac{\partial \phi_0}{\partial t} = \frac{\partial \phi_1}{\partial t}, \quad \frac{\partial \phi_0}{\partial x} = \frac{H_1}{h_1}\frac{\partial \phi_1}{\partial x}, \quad (x = -L), \quad h_1 = H_1 - d(-L), \tag{2.7a}$$

$$\frac{\partial \phi_0}{\partial t} = \frac{\partial \phi_2}{\partial t}, \quad \frac{\partial \phi_0}{\partial x} = \frac{H_2}{h_2}\frac{\partial \phi_2}{\partial x}, \quad (x = L), \quad h_2 = H_2 - d(L). \tag{2.7b}$$

It should be noted that elevation of water surface is not continuous on the boundaries between region S_0 and regions S_1, S_2. At the edges of the plate, the free-edge conditions are satisfied, which imply that the bending moment and shear force are equal to zero:

$$\frac{\partial^2 w}{\partial x^2} = \frac{\partial^3 w}{\partial x^3} = 0, \quad (|x| = L). \tag{2.8}$$

By assuming for simplicity that at initial time the fluid in the region S_2 is at rest, the initial conditions have the form

$$w = w^0(x), \quad \phi_0 = \phi_0^0(x), \quad \eta_1 = \eta_1^0(x), \quad \phi_1 = \phi_1^0(x), \quad \eta_2 = \phi_2 = 0 \quad (t = 0). \tag{2.9}$$

It is also interesting to consider the energy of the plate: the potential energy E_p and the kinetic energy E_k are given by the following integrals (Timoshenko 1959):

$$E_p = \frac{1}{2}\int_{-L}^{L} D(x)\left(\frac{\partial^2 w}{\partial x^2}\right)^2 \mathrm{d}x, \quad E_k = \frac{1}{2}\int_{-L}^{L} m(x)\left(\frac{\partial w}{\partial t}\right)^2 \mathrm{d}x. \tag{2.10}$$

Non-dimensional variables are used below: L is taken as the length scale and $\sqrt{L/g}$ as the time scale.

3. Mode expansions

The plate deflection is sought in the form of an expansion in the eigenfunctions of vibrations of a free-edges homogeneous beam in vacuum

$$w(x,t) = \sum_{n=0}^{\infty} X_n(t) W_n(x). \tag{3.1}$$

Here the functions $X_n(t)$ are to be determined and the functions $W_n(x)$ are solutions of the spectral problem in non-dimensional variables:

$$W_n'''' = \lambda_n^4 W_n \quad (|x| \leqslant 1),$$

$$W_{2n}' = W_{2n+1} = 0 \quad (x = 0), \quad W_n'' = W_n''' = 0, \quad (|x| = 1).$$

The prime denotes differentiation with respect to x. These solutions have the form (Timoshenko 1959):

$$W_0 = 1/\sqrt{2}, \quad W_{2k} = D_{2k}[\cos(\lambda_{2k}x) + S_{2k}\cosh(\lambda_{2k}x)], \quad (k \geqslant 1),$$

$$W_1 = \sqrt{3/2}x, \quad W_{2k+1} = D_{2k+1}[\sin(\lambda_{2k+1}x) + S_{2k+1}\sinh(\lambda_{2k+1}x)], \quad (k \geqslant 1),$$

https://doi.org/10.1017/S0022112009990504 Published online by Cambridge University Press

where $S_n = \cos\lambda_n / \cosh\lambda_n$ and $D_n = 1/\sqrt{1+(-1)^n S_n^2}$. The eigenvalues of λ_n are found from the equation $\tan\lambda_n + (-1)^n \tanh\lambda_n = 0 \quad (n \geqslant 2), \quad \lambda_0 = \lambda_1 = 0$. The functions $W_n(x)$ form a complete orthogonal system for which

$$\int_{-1}^{1} W_n(x) W_m(x)\,\mathrm{d}x = \delta_{mn},$$

where δ_{mn} is the Kronecker symbol.

We substitute expansion (3.1) into (2.1) and initial conditions (2.9), multiply the obtained relations by $W_m(x)$, and integrate them over x from -1 to 1. Using the properties of the functions $W_n(x)$ and integration by parts, we obtain the set of ordinary differential equations (ODEs):

$$\sum_{n=0}^{\infty} [T_{nm}\ddot{X}_n + (\delta_{mn} + P_{nm})X_n] + Z_m(t) = -\Omega_m(t) \quad \text{for} \quad m = 0, 1, 2, \ldots \tag{3.2a}$$

with the initial conditions

$$X_m(0) = X_m^0, \quad \dot{X}_m(0) = X_m^1, \tag{3.2b}$$

where

$$T_{nm} = \int_{-1}^{1} \gamma(x) W_n(x) W_m(x)\,\mathrm{d}x, \quad P_{nm} = \int_{-1}^{1} \beta(x) W_n''(x) W_m''(x)\,\mathrm{d}x, \tag{3.2c}$$

$$Z_m(t) = \int_{-1}^{1} \frac{\partial\phi_0}{\partial t} W_m(x)\,\mathrm{d}x, \quad \Omega_m(t) = \int_{-1}^{1} p(x,t) W_m(x)\,\mathrm{d}x, \tag{3.2d}$$

$$X_m^0 = \int_{-1}^{1} w^0(x) W_m(x)\,\mathrm{d}x, \quad X_m^1 = -\int_{-1}^{1} \left(h(x)\phi_0^{0\prime}(x)\right)' W_m(x)\,\mathrm{d}x, \tag{3.2e}$$

$$\beta(x) = \frac{D(x)}{\rho g L^4}, \quad \gamma(x) = \frac{m(x)}{\rho L},$$

and an overdot denotes differentiation with respect to time. The coefficients T_{nm} and P_{nm} in (3.2c) as well as the functions $\Omega_m(t)$ in (3.2d) can be determined numerically for the given functions $\beta(x)$, $\gamma(x)$ and $p(x,t)$. However, we should find the function $\phi_0(x,t)$ for the determination of the functions $Z_m(t)$.

According to (2.3), a solution for $\phi_0(x,t)$ is sought in the form

$$\phi_0(x,t) = \sum_{n=0}^{\infty} \dot{X}_n(t)\Psi_n(x) + q(x,t), \tag{3.3}$$

where the functions $\Psi_n(x)$ satisfy the equation

$$\Psi_n'(x) = -V_n(x)/h(x), \quad V_n'(x) = W_n(x),$$

and have the form

$$\Psi_n(x) = -\int_{-1}^{x} \frac{V_n(\xi)}{h(\xi)}\,\mathrm{d}\xi, \quad V_0 = \frac{x}{\sqrt{2}}, \quad V_{2k} = \frac{D_{2k}}{\lambda_{2k}}[\sin(\lambda_{2k}x) + S_{2k}\,\sinh(\lambda_{2k}x)],$$

$$V_1 = \frac{\sqrt{3}x^2}{2\sqrt{2}}, \quad V_{2k+1} = \frac{D_{2k+1}}{\lambda_{2k+1}}[S_{2k+1}\,\cosh(\lambda_{2k+1}x) - \cos(\lambda_{2k+1}x)].$$

https://doi.org/10.1017/S0022112009990504 Published online by Cambridge University Press

The unknown function $q(x,t)$ in (3.3) is determined from the equation

$$\frac{\partial}{\partial x}\left(h(x)\frac{\partial q}{\partial x}\right)=0,$$

and has the form

$$q(x,t)=Q(x)u(t)+v(t),\quad Q(x)=\int_{-1}^{x}h^{-1}(\xi)\,\mathrm{d}\xi.$$

The initial conditions for the functions $u(t)$ and $v(t)$ are determined from (2.9), (3.2*b*) and (3.3) as

$$u(0)=u^0,\quad v(0)=v^0, \tag{3.4}$$

where

$$u^0=\frac{1}{\chi}\left[\phi_0^0(1)-\phi_0^0(-1)-\sum_{n=0}^{\infty}X_n^1\Lambda_n\right],\quad v^0=\phi_0^0(-1),\quad \Lambda_n=\Psi_n(1),\quad \chi=Q(1).$$

The functions $u(t)$ and $v(t)$ are determined from the matching conditions (2.7*a*, *b*). In order for these conditions to be used, we should define the forms of the solutions in the regions S_1 and S_2. It is known that an arbitrary localized disturbance in unbounded shallow water over a flat bottom falls into two waves which propagate without deformation with the constant velocity in the opposite directions (Stoker 1957). For the considered problem, the wave of interest propagates along the positive x direction. It is assumed that initially the incoming wave pulse is non-zero only in the region S_1. Its velocity potential can be written as $\psi_0(x-t\sqrt{H_1})$ and the corresponding displacement of the free surface has the form $\zeta_0(x-t\sqrt{H_1})$, where $\zeta_0=\sqrt{H_1}\partial\psi_0/\partial x$. According to the initial conditions (2.9), we have

$$\phi_0^0(x)=\psi_0(x),\quad \eta_1^0(x)=\zeta_0(x).$$

The solution for $\phi_1(x,t)$ is sought in the form

$$\phi_1(x,t)=\psi_0(x-t\sqrt{H_1})+\psi(x,t). \tag{3.5}$$

The function $\psi(x,t)$ defines the velocity potential of the reflected surface waves. According to (2.4), the solution for $\psi(x,t)$ has the form

$$\psi(x,t)=\begin{cases}A((x+1)/\sqrt{H_1}+t), & -(1+\sqrt{H_1}t)<x<-1,\\ 0, & x<-(1+\sqrt{H_1}t),\end{cases} \tag{3.6}$$

where the function $A(\xi)$ is unknown and should be determined. This function is the velocity potential at $x=-1$ for the reflected wave for $t=\xi$.

In a similar manner, we can seek the solution for $\phi_2(x,t)$, which defines the velocity potential of the transmitted surface waves:

$$\phi_2(x,t)=\begin{cases}B(t-(x-1)/\sqrt{H_2}), & 1<x<1+\sqrt{H_2}t,\\ 0, & x>1+\sqrt{H_2}t,\end{cases} \tag{3.7}$$

where the function $B(\xi)$ is to be determined. This function is the velocity potential at $x=1$ for the transmitted wave for $t=\xi$.

https://doi.org/10.1017/S0022112009990504 Published online by Cambridge University Press

By substituting (3.3), (3.5)–(3.7) in the matching conditions (2.7a, b), we obtain sequentially four equations:

$$\dot{A} = \dot{v} + \alpha(t), \tag{3.8a}$$

$$\dot{A} = (u + \dot{X}_0 R_0 - \dot{X}_1 R_1)/\sqrt{H_1} - \alpha(t), \tag{3.8b}$$

$$\dot{B} = \sum_{n=0}^{\infty} \ddot{X}_n \Lambda_n + \chi \dot{u} + \dot{v}, \tag{3.8c}$$

$$\dot{B} = (\dot{X}_0 R_0 + \dot{X}_1 R_1 - u)/\sqrt{H_2}, \tag{3.8d}$$

where $R_n = V_n(1)$, $\alpha(t) = \zeta_0|_{x=-1}$. It can be easily shown that $R_0 = 1/\sqrt{2}$, $R_1 = \sqrt{1.5}/2$, $R_n = 0$ for $n \geqslant 2$. Equations (3.8b) and (3.8d) provide the differential equations for the definition the function $A(t)$ and $B(t)$ with the initial conditions $A(0) = B(0) = 0$. From (3.8a) and (3.8b), we have the equation for $\dot{v}$:

$$\dot{v} = \frac{1}{\sqrt{H_1}}(u + \dot{X}_0 R_0 - \dot{X}_1 R_1) - 2\alpha(t).$$

Using this equation, the functions $Z_m(t)$ in (3.2a, d) have the form

$$Z_m(t) = \int_{-1}^{1} W_m(x) \left[\sum_{n=0}^{\infty} \ddot{X}_n \Psi_n(x) + Q(x)\dot{u} + \dot{v} \right] \mathrm{d}x$$

$$= \sum_{n=0}^{\infty} \ddot{X}_n (\Lambda_n R_m + C_{nm}) + G_m \dot{u} + \sqrt{2}\delta_{m0}\left[(u + \dot{X}_0 R_0 - \dot{X}_1 R_1)/\sqrt{H_1} - 2\alpha\right], \tag{3.9}$$

where

$$C_{nm} = \int_{-1}^{1} \frac{V_n(x) V_m(x)}{h(x)} \mathrm{d}x, \quad G_m = \chi R_m + \Lambda_m.$$

After substitution (3.9) in (3.2a) and application (3.8a–d), the final set of ODEs has the form

$$\sum_{n=0}^{\infty} \left[\left(T_{nm} - \frac{\Lambda_n \Lambda_m}{\chi} + C_{nm} \right) \ddot{X}_n + (\delta_{nm} + P_{nm}) X_n \right] + \left[\frac{G_m}{\chi} \left(\frac{1}{\sqrt{H_2}} - \frac{1}{\sqrt{H_1}} \right) + \sqrt{\frac{2}{H_1}} \delta_{0m} \right] \dot{X}_0 R_0 + \left[\frac{G_m}{\chi} \left(\frac{1}{\sqrt{H_1}} + \frac{1}{\sqrt{H_2}} \right) - \sqrt{\frac{2}{H_1}} \delta_{0m} \right] \dot{X}_1 R_1 + \left[\sqrt{\frac{2}{H_1}} \delta_{0m} - \frac{G_m}{\chi} \times \left(\frac{1}{\sqrt{H_1}} + \frac{1}{\sqrt{H_2}} \right) \right] u + 2 \left(\frac{G_m}{\chi} - \sqrt{2}\delta_{0m} \right) \alpha = -\Omega_m(t) \quad (m = 0, 1, 2, \ldots), \tag{3.10a}$$

$$\dot{u} = \frac{1}{\chi} \left[\left(\frac{1}{\sqrt{H_2}} - \frac{1}{\sqrt{H_1}} \right) \dot{X}_0 R_0 + \left(\frac{1}{\sqrt{H_1}} + \frac{1}{\sqrt{H_2}} \right) (\dot{X}_1 R_1 - u) - \sum_{n=0}^{\infty} \ddot{X}_n \Lambda_n + 2\alpha \right], \tag{3.10b}$$

with initial conditions (3.2b) and (3.4). It should be pointed that this set is a linear set with constant coefficients, which contains two derivatives of X_n, one derivative of u and does not contain v.

Once the $X_n(t)$ and $u(t)$ are determined, we can find all characteristics of motion of the fluid and the elastic plate. For example, the displacement of the free surface of the fluid in region S_1 can be written in view of (3.5) as

$$\eta_1(x, t) = \zeta_0(x - t\sqrt{H_1}) + \zeta(x, t),$$

https://doi.org/10.1017/S0022112009990504 Published online by Cambridge University Press

where

$$\zeta(x,t)=\begin{cases}-\dot{A}((x+1)/\sqrt{H_1}+t), & -(1+\sqrt{H_1}t)<x<-1,\\ 0, & x<-(1+\sqrt{H_1}t).\end{cases}$$

In region S_2, we have

$$\eta_2(x,t)=\begin{cases}-\dot{B}(t-(x-1)/\sqrt{H_2}), & 1<x<1+\sqrt{H_2}t,\\ 0, & x>1+\sqrt{H_2}t.\end{cases}$$

The functions $\dot{A}(\xi)$ and $\dot{B}(\xi)$ are determined from (3.8*b*) and (3.8*d*).

The energy of reflected wave motion $E_r(t)$ (the sum of the potential and kinetic energies) is equal to (Stoker 1957)

$$E_r(t)=\int_{-(1+\sqrt{H_1}t)}^{-1}\zeta^2(x,t)\,\mathrm{d}x=\sqrt{H_1}\int_0^t\dot{A}^2(\xi)\,\mathrm{d}\xi. \tag{3.11}$$

The energy of transmitted wave motion $E_t(t)$ is equal to

$$E_t(t)=\int_1^{1+\sqrt{H_2}t}\eta_2^2(x,t)\,\mathrm{d}x=\sqrt{H_2}\int_0^t\dot{B}^2(\xi)\,\mathrm{d}\xi. \tag{3.12}$$

Using the reduction method, we replace the infinite series in the expansion (3.1) by the finite sum with number of terms N. Equation (3.10*a*) can be written in the matrix form

$$\boldsymbol{A}\ddot{\boldsymbol{X}}+\boldsymbol{B}\dot{\boldsymbol{X}}+\boldsymbol{D}\boldsymbol{X}+\boldsymbol{F}u=\boldsymbol{G}, \tag{3.13}$$

where $\boldsymbol{A}$, $\boldsymbol{B}$, $\boldsymbol{C}$ are the square matrices of order N, but $\boldsymbol{X}$, $\boldsymbol{D}$, $\boldsymbol{F}$, $\boldsymbol{G}$ are the vectors, the vector $\boldsymbol{X}=\{X_0,X_1,\ldots,X_{N-1}\}^T$, and the superscript T is denoted the transposition. After inversion of the symmetric matrix $\boldsymbol{A}$ in (3.13), we have

$$\ddot{\boldsymbol{X}}=\boldsymbol{A}^{-1}(\boldsymbol{G}-\boldsymbol{B}\dot{\boldsymbol{X}}-\boldsymbol{D}\boldsymbol{X}-\boldsymbol{F}u). \tag{3.14}$$

By substituting (3.14) in (3.10*b*), we can write the final set of ODEs in the matrix form

$$\dot{\boldsymbol{Y}}=\boldsymbol{C}\boldsymbol{Y}+\boldsymbol{H}(t), \tag{3.15}$$

where the vector $\boldsymbol{Y}=\{\boldsymbol{X},\dot{\boldsymbol{X}},u\}^T$, $\boldsymbol{C}$ is the square matrix of order $2N+1$ with the constant coefficients which depend only on the properties of the plate and the fluid and independent of the wave forcing, whereas the vector $\boldsymbol{H}(t)$ is determined by the unsteady load.

The solution of reduced set of ODEs (3.10*a*, *b*) in the matrix form (3.15) can be numerically obtained by two ways: the time-stepping procedure and the calculation of the eigenvalues and the eigenvectors of the matrix $\boldsymbol{C}$. The second way is better because it is possible to write the explicit solution for any wave forcing (see, for example, Godunov 1997). The knowledge of the eigenvalues allows to predict also the peak response of the plate for the harmonically forced vibration.

4. Action of periodic surface pressures

The problem of the behaviour of an elastic floating plate under the action of periodic surface load is related to the problem for a single frequency. In contrast to the diffraction problem, the effect of periodic load is studied in a small body of literature. Apart from the paper by Meylan (1997) which has been mentioned in Introduction, the action of periodic load was considered by Sturova (2002*a*) for

https://doi.org/10.1017/S0022112009990504 Published online by Cambridge University Press

a plate of finite and semi-infinite breadth in the two-dimensional case and for a circular plate in the three-dimensional case. A vertical mode expansion was used. The solutions obtained for a fluid of finite depth and for shallow water were compared. The two-dimensional problem was studied by Tkacheva (2005*a*) for a fluid of finite depth using the Wiener–Hopf technique. This technique was also applied to the problem of the behaviour of a floating elastic plate under periodic vibrations of a bottom section (Tkacheva 2005*b*). The action of periodic pressure on an elastic plate floating on the surface of an infinitely deep fluid was considered by Sturova & Korobkin (2005) using the expansion in terms of modal functions of a beam with free edges conditions. The behaviour of wave motion generated by periodic pressure on a rectangular elastic plate was considered within the shallow-water theory in Sturova (2006*a*). The boundary-integral-equation method was applied. It was shown that waveguide properties occur for an elongated plate. The existence of trapped mode solution for an elastic strip was found out by Tkacheva (2000).

All mentioned models about a periodic load supposed the homogeneous elastic plate over a bed that is either flat or infinitely deep. Let us consider the hydroelastic behaviour of a heterogeneous plate floating on shallow water of variable depth. A time-periodic pressure with frequency ω acts on the plate. The single-frequency equations are based on assuming that all time-dependent quantities in (2.1) are proportional to $\mathrm{e}^{\mathrm{i}\omega t}$, so that

$$p(x,t) = \mathrm{Re}[P(x)\mathrm{e}^{\mathrm{i}\omega t}], \quad w(x,t) = \mathrm{Re}[W(x)\mathrm{e}^{\mathrm{i}\omega t}], \tag{4.1a}$$

$$\phi_j(x,t) = \mathrm{Re}[\Phi_j(x)\mathrm{e}^{\mathrm{i}\omega t}], \quad (j = 0, 1, 2). \tag{4.1b}$$

Then (2.1) and (2.3) can be written in non-dimensional variables as

$$(\beta(x)W'')'' + W[1 - \omega^2\gamma(x)] + \mathrm{i}\omega\Phi_0 = -P(x), \tag{4.2a}$$

$$W = \frac{\mathrm{i}}{\omega}\left(h(x)\Phi_0'\right)'. \tag{4.2b}$$

It is assumed that the others sources of the wave forcing are absent.

In the free-water regions, we have from (2.4):

$$\Phi_j = -H_j\Phi_j''/\omega^2 \quad (x \in S_j), \quad (j = 1, 2). \tag{4.3}$$

Far from the plate, it is necessary to take account of the radiation condition

$$\Phi_1' - \mathrm{i}k_1\Phi_1 = 0 \quad (x \to -\infty), \quad k_1 = \omega/\sqrt{H_1}, \tag{4.4a}$$

$$\Phi_2' + \mathrm{i}k_2\Phi_2 = 0 \quad (x \to \infty), \quad k_2 = \omega/\sqrt{H_2}. \tag{4.4b}$$

The matching conditions and the free-edge conditions should be added at $|x| = 1$ by analogy with (2.7*a*, *b*) and (2.8).

According to (4.3) and the radiation condition (4.4*a*, *b*), the solutions for $\Phi_1(x)$ and $\Phi_2(x)$ can be written as

$$\Phi_1(x) = A\mathrm{e}^{\mathrm{i}k_1 x}, \quad \Phi_2(x) = B\mathrm{e}^{-\mathrm{i}k_2 x}, \tag{4.5}$$

where the complex constants A and B are unknown and should be determined. Using the expansion of the plate motion in the free modes, we have by analogy with (3.1)

$$W(x) = \sum_{n=0}^{\infty} X_n W_n(x), \tag{4.6}$$

https://doi.org/10.1017/S0022112009990504 Published online by Cambridge University Press

where X_n are unknown complex constants now. For the problem of a single frequency, the set of ODEs (3.10a, b) is reduced to the set of linear algebraic equations for X_n.

It is of interest to determine averaged over the period $2\pi/\omega$ the values of the potential energy and the kinetic energy. Using (2.10) and (4.1a), we have in non-dimensional variables

$$E_p = \frac{1}{2}\int_{-1}^{1} \beta(x)[\mathrm{Re}(W'')\cos\omega t - \mathrm{Im}(W'')\sin\omega t]^2\,\mathrm{d}x, \tag{4.7a}$$

$$E_k = \frac{\omega^2}{2}\int_{-1}^{1} \gamma(x)[\mathrm{Re}(W)\sin\omega t + \mathrm{Im}(W)\cos\omega t]^2\,\mathrm{d}x. \tag{4.7b}$$

Averaged values of the potential energy $\langle E_p\rangle$ and the kinetic energy $\langle E_k\rangle$ can be written with regard to (3.2c) and (4.6) as

$$\langle E_p\rangle = \frac{1}{4}\sum_{m=0}^{\infty}\sum_{n=0}^{\infty}\Upsilon_{mn}P_{mn}, \quad \langle E_k\rangle = \frac{\omega^2}{4}\sum_{m=0}^{\infty}\sum_{n=0}^{\infty}\Upsilon_{mn}T_{mn}, \tag{4.8}$$

where $\Upsilon_{mn} = \mathrm{Re}(X_m)\mathrm{Re}(X_n) + \mathrm{Im}(X_m)\mathrm{Im}(X_n)$.

5. Numerical results

The physical properties for ice sheet are used in all of the results presented in this section (see, for example, Bennetts, Biggs & Porter 2007). The flexural rigidity of the ice sheet is equal to (returning to the dimensional variables)

$$D(x) = \frac{E F^3(x)}{12(1-\nu^2)},$$

where $E = 5\times10^9$ Pa is Young's modulus for ice, $F(x)$ is its varying thickness and $\nu = 0.3$ is Poisson's ratio for ice. The mass per unit length of the ice sheet is equal to $m(x) = \rho_1 F(x)$, where $\rho_1 = 922.5$ kg m^{-3} is the ice density. For simplicity assume that each segment of the ice would be neutrally buoyant, i.e. $d(x) = \rho_1 F(x)/\rho$, the density of the water $\rho = 1025$ kg m^{-3}. In this case (2.2) is fulfilled identically.

The width of the ice sheet is equal to $2L = 500$ m. The ice thickness is given by the functions

$$F(x) = F_0 + A_D\left(1 - \frac{|x|}{L}\right), \tag{5.1}$$

$$F(x) = F_0 + \frac{A_D}{2}\left(1 + \frac{x}{L}\right). \tag{5.2}$$

The first function represents local bulge in the ice of size $F_0 + A_D$ in the middle of the ice sheet, whereas the second function represents a linear increase in ice thickness over the interval $(-L, L)$.

Four different variations of sea-bottom topography are considered: the hump, the pit and two kinds of the slope. The profile which is described by the function

$$H(x) = H_1 + H_D\left[\left(\frac{x}{L}\right)^2 - 1\right] \tag{5.3}$$

https://doi.org/10.1017/S0022112009990504 Published online by Cambridge University Press

at $H_1 = H_2$ corresponds to the hump at $H_D > 0$ and the pit at $H_D < 0$. The depth of water rises linearly for the slopes

$$H(x) = (H_2 - H_1)\frac{x}{L} + H_2 \quad (-L < x < 0), \quad H(x) = H_2 \quad (0 < x < L), \tag{5.4}$$

$$H(x) = \frac{1}{2}\left[(H_2 - H_1)\frac{x}{L} + H_1 + H_2\right]. \tag{5.5}$$

The first one (slope I) is that the bottom varies linearly from the left edge of floating plate to the middle of that. The second one (slope II) is that it varies linearly from the left edge to the right one.

The infinite series in the expansions (3.1) and (4.6) are replaced with a sum of N terms. In all presented calculations, $N = 30$, and further increase of N gives graphically indistinguishable results in the figures presented below. The set of ODEs (3.10a, b) in the matrix form (3.15) is solved using both the fourth-order Runge–Kutta scheme and the explicit solution with the eigenvalues/eigenvectors. The coefficients C_{nm}, P_{nm}, T_{nm}, Λ_n and χ are determined using numerical integration.

For the problem of the scattering of localized surface wave by an elastic plate, the incoming wave was chosen in the form

$$\zeta_0(\xi) = \begin{cases} 0.5a[1 + \cos(\pi\xi/c)], & |\xi| < c, \\ 0, & |\xi| > c, \end{cases}$$

where $\xi = x - t\sqrt{gH_1} - x_0$, and x_0 is the initial location of the wave peak. In all of the presented results we use $x_0/L = -1.25$, and $c/L = 0.25$. Total energy of this wave E_0 (the sum of the potential energy and the kinetic energy) is equal to (Stoker 1957)

$$E_0 = \rho g \int_{-c}^{c} \zeta_0^2(\xi)\,\mathrm{d}\xi = 3\rho g a^2 c/4. \tag{5.6}$$

Notice that for this wave, the potential energy is equal to the kinetic energy.

It is assumed, that at the initial time the plate and fluid in the regions S_0 and S_2 are at rest, and the external load is absent. By this is meant that $w^0(x) = \phi_0^0(x) = 0$ in (2.9) and $p(x, t) = 0$ in (2.1). In region S_1, the localized displacement of the free surface travels to the right. At $t = 0$ this wave reaches the left edge of the plate and the plate begins to undergo a complex bending motion in response to the incoming wave. As $t \to \infty$, the plate oscillations decay and the plate returns to its original state. The energies of reflected and transmitted surface waves are determined in (3.11) and (3.12). Since dissipation is absent in the considered problem, we have in accordance with (5.6)

$$\lim_{t\to\infty}[E_r(t) + E_t(t)] = E_0. \tag{5.7}$$

The fulfilment of this equality is a criterion of the accuracy of the method of solution used.

Figure 2 shows the displacements of the free surface (the thin lines) and the elastic plate (the bold lines) for a surface localized wave travelling to the right at the time $t\sqrt{g/L} = 0, 1.5, 3, 4.5, 6, 7.5, 9, 10.5$ and 12. The ice thickness is given by (5.1) with $F_0 = 1$ m and $A_D = 2$ m. The bottom topography has the form of the hump (5.3) with $H_1 = 20$ m and $H_D = 10$ m. At $t = 0$ the plate is at rest and the wave is to the left of plate propagating towards it. Then the incoming wave passes under the plate, that leads to its bending motion. The response of the plate in turn induces waves in the surrounding water which propagate away from the plate to the left and right. The

https://doi.org/10.1017/S0022112009990504 Published online by Cambridge University Press

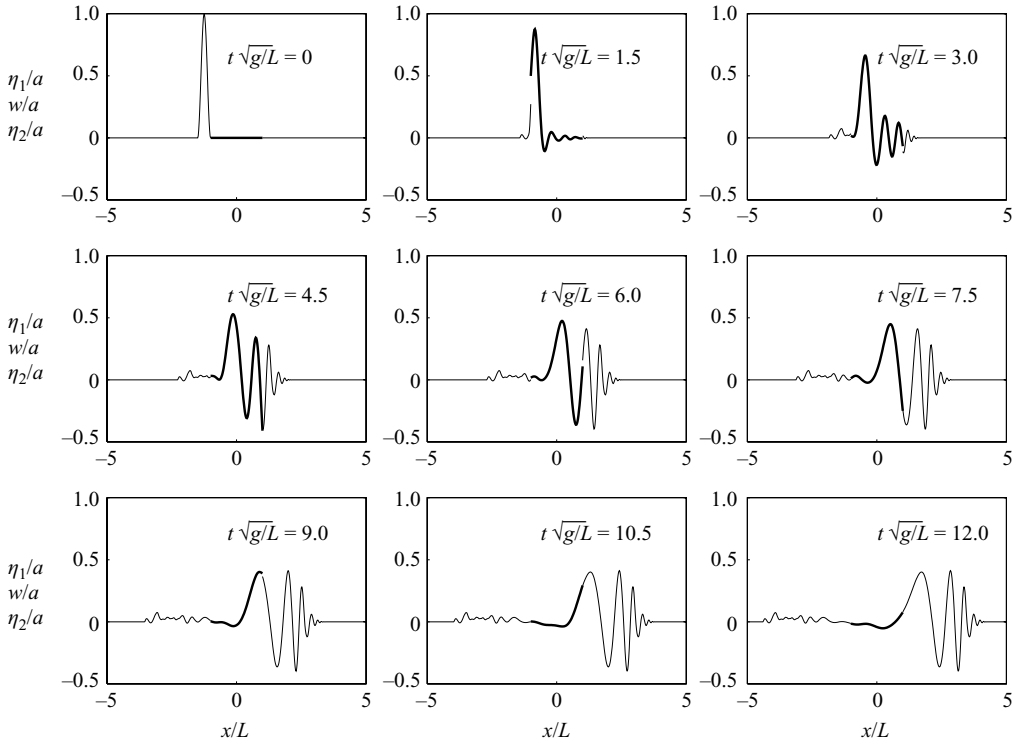


FIGURE 2. The time evolution of the free surface (the thin lines) and the plate (the bold lines) due to a localized surface wave travelling to the right is shown. The function $F(x)$ is given by (5.1), with $F_0 = 1$ m and $A_D = 2$ m. The function $H(x)$ is given by (4.3), with $H_1 = 2H_D = 20$ m.

final picture, $t\sqrt{g/L} = 12$, shows the plate approaching the state of rest, with waves now propagating away from it. The majority of the wave energy has passed under the plate and continues to propagate to the right. However, the shape of the outgoing wave profile is markedly different from the incoming wave profile. Also, there is an appreciable reflected wave propagating away from the plate to the left.

The comparison of the displacements of the free surface and the elastic plate for the homogeneous and heterogeneous plates with different topographies is presented in figure 3 at the times $t\sqrt{g/L} = 6$ (a–c) and $t\sqrt{g/L} = 12$ (d–f). Figures 3(a) and 3(d) correspond to the homogeneous plate with the function $F(x) = F_0 = 1$ m and the flat bottom with the depth $H_1 = 20$ m. Figures 3(b) and 3(e) also correspond to the flat bottom, but the ice thickness is given by (5.1) with $F_0 = 1$ m and $A_D = 2$ m. The same ice thickness is used for figures 3(c) and 3(f), but the bottom topography has the form of the pit with $H_1 = 20$ m and $H_D = -10$ m.

A comparison between figures 3 and 2 for the times $t\sqrt{g/L} = 6, 12$ shows that the behaviour of the elastic plate and the free surface is conditioned significantly by both the plate properties and the bed shapes. It should be noted that at $t\sqrt{g/L} = 12$ the plate is practically at rest for the flat bottom and the pit; however, there are still noticeable deflections of the plate for the hump.

Time variations of the sum $E(t) = E_r(t) + E_t(t)$ are presented in figure 4 for the same cases as in figures 2 and 3. The limiting value of the summarized energy is achieved most rapidly in the case of the pit. Therefore, the plate oscillations are damped in

https://doi.org/10.1017/S0022112009990504 Published online by Cambridge University Press

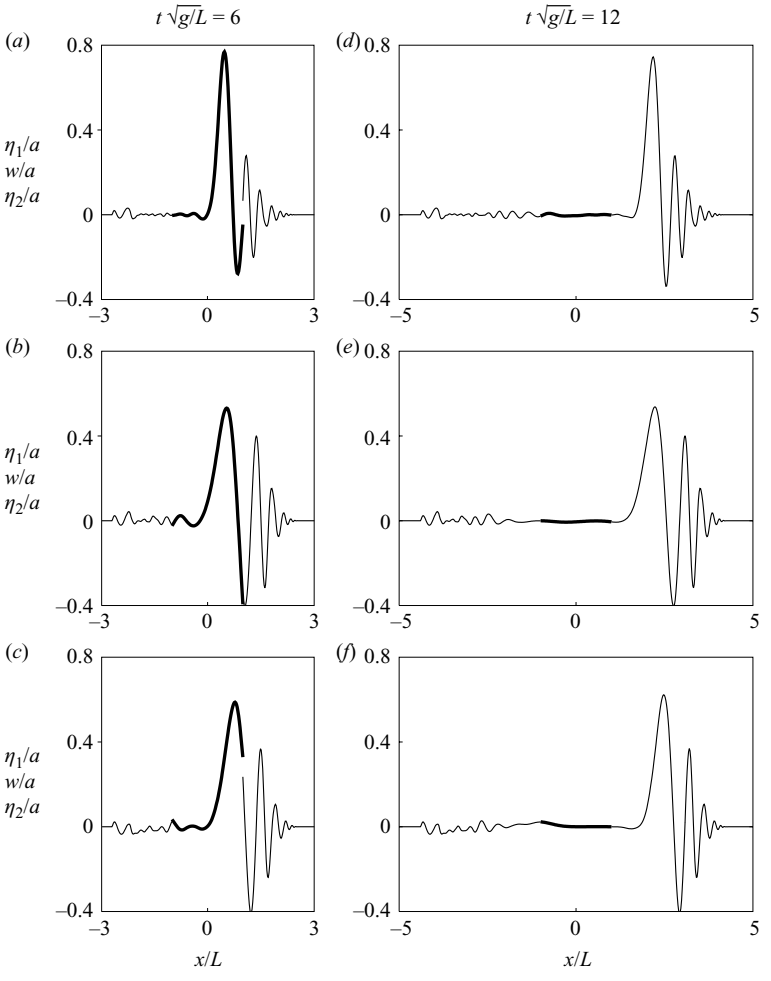


FIGURE 3. Comparison of the behaviour of free surface (the thin lines) and the plate (the bold lines) at $t\sqrt{g/L}=6$ (*a–c*) and $t\sqrt{g/L}=12$ (*d–f*). (*a*) and (*d*), $F(x)=F_0=1$ m and $H(x)=H_1=20$ m; (*b*) and (*e*), $F_0=1$ m, $A_D=2$ m and $H(x)=H_1=20$ m; (*c*) and (*f*), $F_0=1$ m, $A_D=2$ m and the bed shape (5.3) with $H_1=20$ m, $H_D=-10$ m.

this case more effectively then for three other cases. The most prolonged oscillations take place in the presence of the hump. For all cases the total energy of the reflected waves $E_r(t)$ is low and does not exceed $0.02E_0$.

In figure 5, the effect both of the ice thickness given by (5.2) with $F_0=1$ m, $A_D=2$ m and the bed shapes (5.4), (5.5) with $H_1=20$ m, $H_2=10$ m is investigated for the times $t\sqrt{g/L}=6$ (*a–c*) and $t\sqrt{g/L}=12$ (*d–f*). As in figures 2 and 3, the behaviour of the elastic plate and the free surface is conditioned significantly by both the plate heterogeneity and the bottom topography. Time evolution of the summarized energy $E(t)$ for these cases is shown in figure 6. The limiting value of the summarized energy is achieved most rapidly in the case of the flat bottom. The most prolonged oscillations take place in the presence of the slope I. In this case we have also the highest value of the total energy of the reflected waves $E_r(t)$, which runs up to $0.04E_0$.

https://doi.org/10.1017/S0022112009990504 Published online by Cambridge University Press

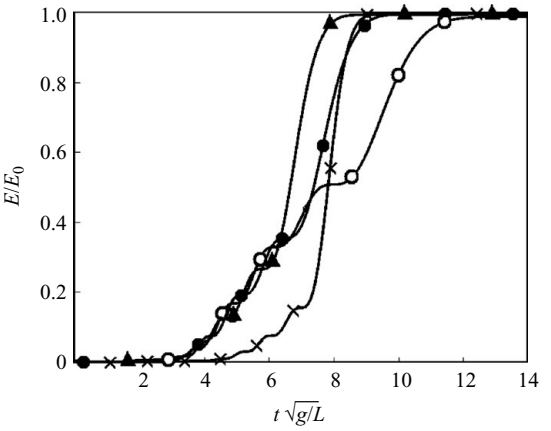


FIGURE 4. Time variation of the energy of surface waves. The lines with symbols correspond to: the crosses, $F(x) = F_0 = 1$ m and $H(x) = H_1 = 20$ m; the dark circles, $F_0 = 1$ m, $A_D = 2$ m and $H(x) = H_1 = 20$ m; the open circles, $F_0 = 1$ m, $A_D = 2$ m and the bed shape (5.3) with $H_1 = 20$ m, $H_D = 10$ m; the triangles, $F_0 = 1$ m, $A_D = 2$ m and the bed shape (5.3) with $H_1 = 20$ m, $H_D = -10$ m.

The relative error of the fulfilment of the equality (5.7) does not exceed 0.5 % for all calculations which are presented in figures 2–6.

Next, we consider the plate behaviour caused by its initial deformation in the fluid at rest. The initial plate velocity is equal to zero and the external load is absent. Now, we have $\phi_0^0(x) = \eta_1^0(x) = \phi_1^0(x) = 0$ in (2.9) and $p(x, t) = 0$ in (2.1). The set of ODEs for the solution of this problem coincides with (3.10a, b) provided that now $\alpha(t) \equiv 0$. The function $w^0(x)$ in (2.9) is chosen in the form

$$w^0(x) = \frac{a}{2}\left(1 + \cos\frac{\pi x}{L}\right).$$

The deflections of the heterogeneous ice plate induced by its initial displacement are shown in figure 7 at the time $t\sqrt{g/L} = 0, 1.5, 3, 4.5, 6$ and 7.5. The ice thickness is given by (5.2) with $F_0 = 1$ m, $A_D = 2$ m. The solid lines correspond to the flat bottom with $H(x) = H_1 = 20$ m, the dashed lines and the dash-dotted ones correspond to the bed shapes (5.4) and (5.5), respectively, with $H_1 = 20$ m, $H_2 = 10$ m. The initial deformation disappears with time and the plate tends to a horizontal unperturbed position. The plate oscillations attenuate more rapidly for the fluid with the constant depth. The most prolonged oscillations take place for the slope I.

Of some interest in the considered problem is the analysis of the eigenvalues of the matrix $\boldsymbol{C}$ in (3.15), which can be determined by numerically. This matrix has one pure real eigenvalue μ_0 and $2N$ complex conjugate eigenvalues μ_j ($j = \pm 1, \pm 2, \ldots, \pm N$). The real part of all eigenvalues is negative due to the radiation of energy with surface waves. The eigenvalues are ordered by increasing imaginary part, i.e. $\mathrm{Im}\mu_j < \mathrm{Im}\mu_{j+1}$. The sign of j corresponds to the sign of the imaginary part of the eigenvalue μ_j.

Figure 8 shows the location of the eigenvalues μ_j at $j = 0, 1, \ldots, J$, where J is defined from the condition $\mathrm{Im}\mu_j\sqrt{L/g} < 10$. Figure 8($a$) corresponds to the flat bottom and the different heterogeneities of the ice plate, whereas figure 8(b) shows the effect of the bed shape for the heterogeneous plate. We can see that both the heterogeneity of the plate and the bottom topography have an appreciable effect on the distribution of the eigenvalues. The time history of the plate motion is determined

https://doi.org/10.1017/S0022112009990504 Published online by Cambridge University Press

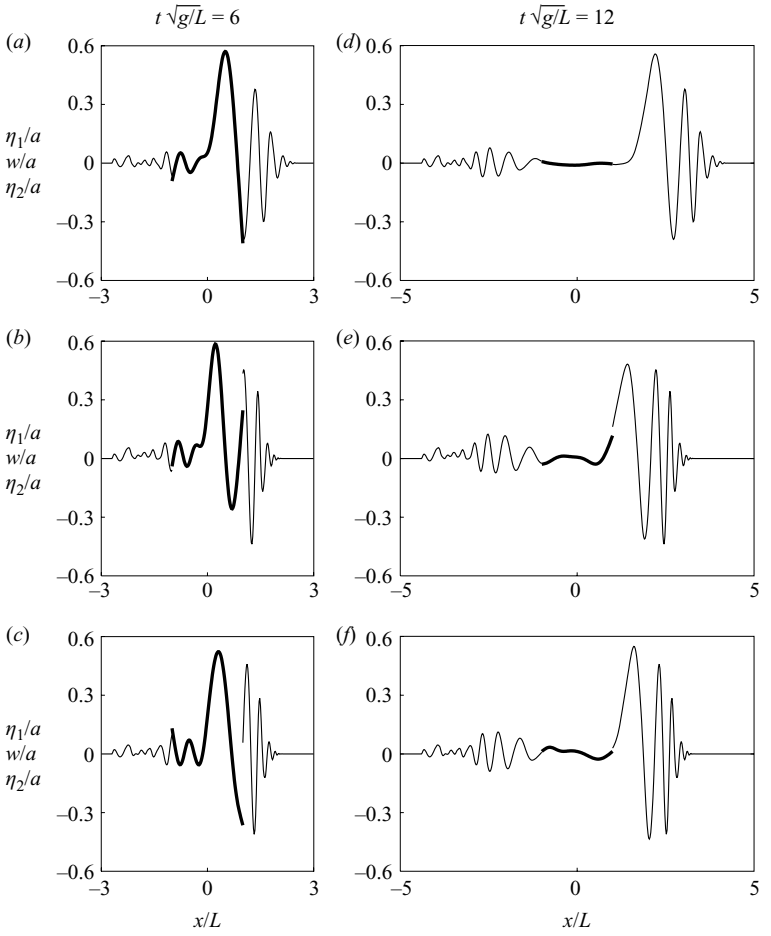


FIGURE 5. As for figure 3 except that the ice thickness given by (5.2) with $F_0 = 1$ m, $A_D = 2$ m: (*a*) and (*d*), $H(x) = H_1 = 20$ m; (*b*) and (*e*), the bed shape (5.4) with $H_1 = 2H_2 = 20$ m; (*c*) and (*f*), the bed shape (5.5) with $H_1 = 2H_2 = 20$ m.

basically by the lower eigenvalues because these eigenvalues have the larger real parts. Among the considered cases the largest real part takes place for the heterogeneous plate with the ice thickness given by (5.2) with $F_0 = 1$ m, $A_D = 2$ m and the bed shape in the form of slope I that provides the most prolonged oscillations of the plate in this case (cf. figures 5–7).

It should be pointed out that the determination of the eigenvalues is very important for the single-frequency solutions. As noted in Meylan (2001), from a knowledge of the eigenvalues we can predict the frequencies for which the response of the floating elastic plate is maximum in the diffraction problem. The imaginary parts of the eigenvalues allow us to find the real frequencies at which the transmission coefficient is unity and the reflection is zero. Meylan (2001, 2002) calculated the eigenvalues for the typical input data of a large floating structure such as a floating runway. It was assumed that the homogeneous elastic plate floats on shallow water of the constant depth. He used a complex search algorithm based on the properties of contour integrals of analytical functions. This search algorithm was much more numerically

https://doi.org/10.1017/S0022112009990504 Published online by Cambridge University Press

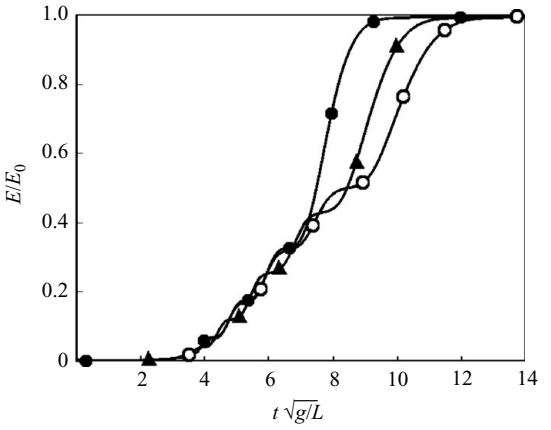


FIGURE 6. As for figure 4 except that the ice thickness given by (5.2) with $F_0 = 1$ m and $A_D = 2$ m. The lines with symbols correspond to: the dark circles, $H(x) = H_1 = 20$ m; the open circles, the bed shape (5.4) with $H_1 = 2H_2 = 20$ m; the triangles, the bed shape (5.5) with $H_1 = 2H_2 = 20$ m.

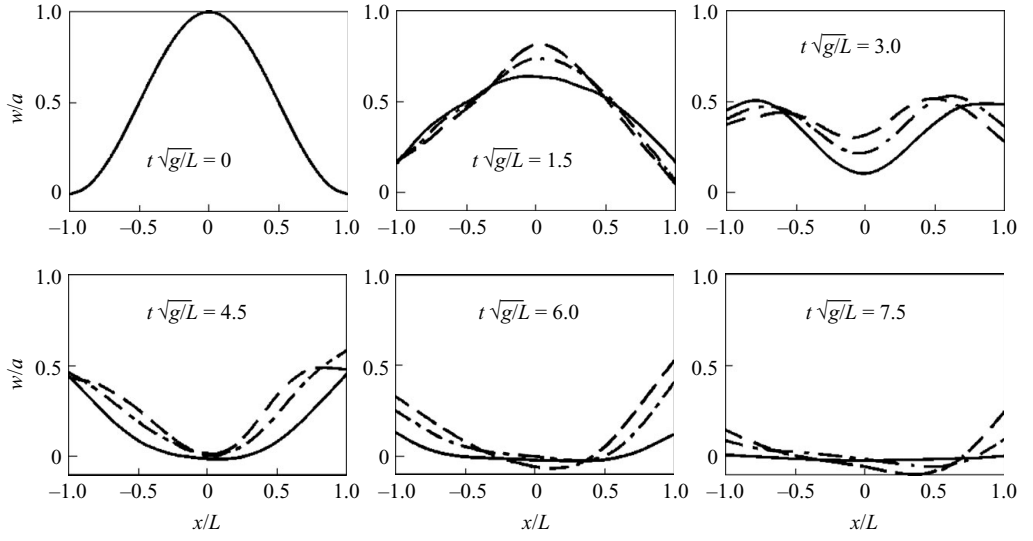


FIGURE 7. The evolution of the elastic plate caused by its initial deformation for the ice thickness given by (5.2) with $F_0 = 1$ m and $A_D = 2$ m. The solid lines are for the flat bottom with $H(x) = H_1 = 20$ m, the dashed lines are for the bed shape (5.4) and the dash-dotted lines are for the bed shape (5.5) with $H_1 = 2H_2 = 20$ m.

difficult than the matrix eigenvalue problem we solve here to find these points. A correlation was made between the results by Meylan (2001, 2002) and the results of the proposed method. Good agreement is obtained with the only difference that the real part of the eigenvalues of this paper corresponds to the imaginary part of Meylan's papers and vice versa. Also good agreement is obtained at the comparison of the behaviour of the elastic plate and free surface for the unsteady problems which were considered by Meylan (2002).

The interrelation between the eigenvalues and the peak response of the plate has now been demonstrated with the problem on the action of a periodic load. The

https://doi.org/10.1017/S0022112009990504 Published online by Cambridge University Press

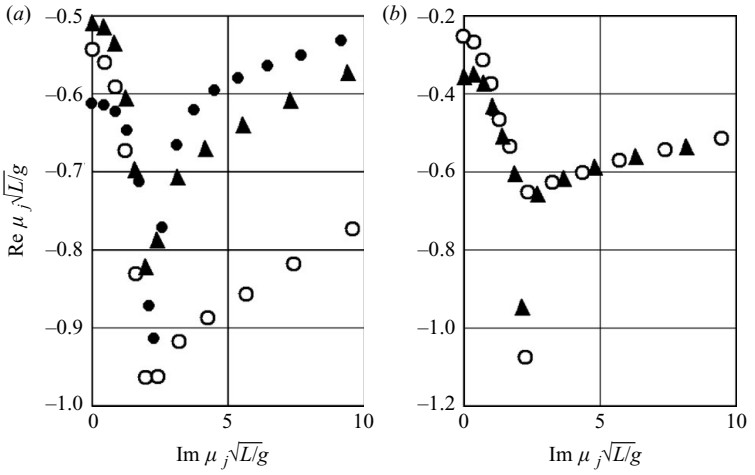


FIGURE 8. The location of the first eigenvalues. (*a*) The flat bottom with $H(x) = H_1 = 20$ m; the dark circles, the homogeneous ice plate with $F(x) = F_0 = 1$ m; the open circles, the heterogeneous ice plate with the ice thickness given by (5.1) with $F_0 = 1$ m and $A_D = 2$ m; the triangles, the heterogeneous ice plate with the ice thickness given by (5.2) with $F_0 = 1$ m and $A_D = 2$ m. (*b*) The heterogeneous ice plate with the ice thickness given by (5.2) with $F_0 = 1$ m and $A_D = 2$ m: the open circles, the bed shape given by (5.4); the triangles, the bed shape given by (5.5), both with $H_1 = 2H_2 = 20$ m.

following pressure distribution is used in (4.2*a*):

$$P(x) = \begin{cases} a\rho g\left[1 - (x - x_0)^2/c^2\right], & |x - x_0| < c, \\ 0, & |x - x_0| > c, \end{cases} \tag{5.8}$$

where a has a dimension of the length and $|x_0| + c < L$. Figure 9(*a*) shows the non-dimensional values of the averaged potential energy $\bar{E}_p = \langle E_p \rangle/(a^2\rho g L)$, the averaged kinetic energy $\bar{E}_k = \langle E_k \rangle/(a^2\rho g L)$ and their sum $\bar{E}_s = \bar{E}_p + \bar{E}_k$ as a function of the frequency at $x_0/L = 0.75$ and $c/L = 0.1$. The ice thickness is given by (5.2) with $F_0 = 1$ m, $A_D = 2$ m and the bed shape given by (5.5) with $H_1 = 20$ m, $H_2 = 10$ m. The stars show the imaginary part of the eigenvalues (cf. figure 8*b*). We can see that the value of the potential energy significantly greater than the value of the kinetic energy. The frequency dependence of the potential energy as well as the kinetic one is extremely non-monotonic. The peaks occur at the frequencies which correspond to the imaginary part of the eigenvalues. The frequency dependence of the total energy $\bar{E}_s$ for the various values x_0 and c is shown in figure 9(*b*). The solid, dash-dotted and dotted lines correspond to $c/L = 0.1$ with $x_0/L = 0,\ 0.25,\ 0.5$, respectively, and the dashed line corresponds to $x_0/L = 0.75$ and $c/L = 0.05$. As seen from the figures 9(*a*) and 9(*b*), the distribution of the total energy $\bar{E}_s$ with frequency essentially depends on the location and the form of the external load. A knowledge of the eigenvalues/eigenvectors of the considered problem and the methods of the theory of vibrations (see, for example, Müller & Schiehlen 1985) allow to determine the frequencies which produce the maximal response of the floating plate for the given pressure.

https://doi.org/10.1017/S0022112009990504 Published online by Cambridge University Press

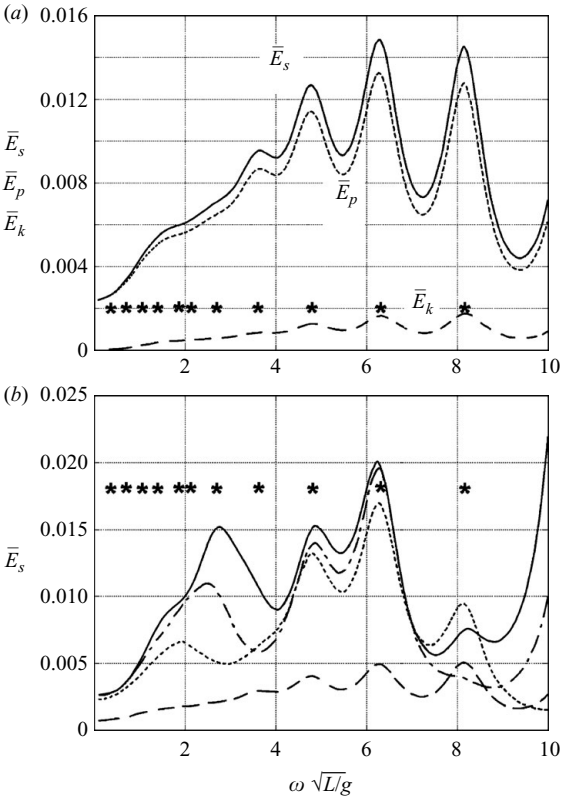


FIGURE 9. Averaged energy of the plate as a function of frequency for the heterogeneous ice plate with the ice thickness given by (5.2) at $F_0 = 1$ m and $A_D = 2$ m and the bed shape given by (5.5) at $H_1 = 2H_2 = 20$ m. The stars show the imaginary part of the eigenvalues. (*a*) The pressure distribution (5.8) with $x_0/L = 0.75$ and $c/L = 0.1$. The solid, dotted and dashed lines correspond to the total energy $\bar{E}_s$, the potential energy $\bar{E}_p$ and the kinetic energy $\bar{E}_k$, respectively. (*b*) The solid, dash-dotted and dotted lines correspond to $c/L = 0.1$ with $x_0/L = 0,\ 0.25,\ 0.5$, respectively, and the dashed line corresponds to $x_0/L = 0.75$ and $c/L = 0.05$.

6. Conclusion

The time-domain mode-expansion method is developed for hydroelastic analysis of the heterogeneous plate floating on shallow water of variable depth. Numerical simulations are carried out for three unsteady problems: the scattering of localized surface wave by a plate, decay of the initial displacement of the plate and action of a periodic load on a plate. Effects of both the uneven bottom and the structural heterogeneity of the floating plate are considered. It is shown that both these effects have a profound impact on the plate deflections and wave motion of the fluid. The sea-bottom effects should be considered when the floating structure is placed in the coastal area. The simple easy-to-use model applied in this study captures the main characteristics of the complex problem of unsteady hydroelasticity. The proposed method can be extended to the case of a circular plate subject to the condition that the bottom undulations are located only beneath the plate. Unsteady behaviour of a homogeneous circular plate floating on shallow water with a flat bottom has been presented in Sturova (2003).

https://doi.org/10.1017/S0022112009990504 Published online by Cambridge University Press

This study was partially supported by RFBR (07-08-00145) and the Foundation 'Leading Scientific Schools' (NSh-2260.2008.1). I am grateful to the Journal's reviewers, whose constructive comments helped improve the quality of the presentation.

REFERENCES

Bennetts, L. G., Biggs N. R. T. & Porter, D. 2007 A multi-mode approximation to wave scattering by ice sheets of varying thickness. *J. Fluid Mech.* **579**, 413–443.

Chen, X.-J., Wu Y.-S., Cui, W.-C. & Jensen, J. J. 2006 Review of hydroelasticity theories for global response of marine structures. *Ocean Engng* **33**, 439–457.

Endo, H. & Yago, K. 1999 Time history response of a large floating structure subjected to dynamic load. *J. Soc. Nav. Archit. Japan* **186**, 369–376.

Godunov, S. K. 1997 *Ordinary Differential Equations with Constant Coefficient*. Translations of Mathematical Monographs, vol. 169. American Mathematical Society, Providence, RI.

Hazard, C. & Meylan, M. H. 2007 Spectral theory for an elastic thin plate floating on water of finite depth. *SIAM J. Appl. Math.* **68**, 629–647.

Kashiwagi, M. 2000 A time-domain mode-expansion method for calculating transient elastic responses of a pontoon-type VLFS. *J. Mar. Sci. Technol.* **5**, 89–100.

Kashiwagi, M. 2004 Transient responses of a VLFS during landing and take-off of an airplane. *J. Mar. Sci. Technol.* **9**, 14–23.

Lee, D. H. & Choi, H. S. 2003 Transient hydroelastic response of very large floating structures by FE-BE hybrid method. In *Proceedings of the Thirteenth International Society of Offshore and Polar Engineering, Honolulu, Hawaii, USA*, May 2003, pp. 100–105.

Meylan, M. H. 1997 The forced vibration of a thin plate floating on an infinite liquid. *J. Sound Vib.* **205**, 581–591.

Meylan, M. H. 2001 An application of scattering frequencies to hydroelasticity. In *Proceedings of the Eleventh International Society of Offshore and Polar Engineering, Stavanger, Norway*, June 2001. Intern. Society of Offshore and Polar Engineers, Cupertino, California, vol. 3, pp. 385–391.

Meylan, M. H. 2002 Spectral solution of time-dependent shallow water hydroelasticity. *J. Fluid Mech.* **454**, 387–402.

Müller, P. C. & Schiehlen, W. O. 1985 *Linear Vibrations*. Martinus Nijhoff Publishers.

Ohmatsu, S. 1998 Numerical calculation of hydroelastic behaviour of VLFS in time domain. In *Proceedings of the Second International Conference on Hydroelasticity in Marine Technology, Fukuoka, Japan*, December 1998, pp. 89–97.

Ohmatsu, S. 2005 Overview: research on wave loading and responses of VLFS. *Mar. Struct.* **18**, 149–168.

Porter, D. & Porter, R. 2004 Approximations to wave scattering by an ice sheet of variable thickness over undulating bed topography. *J. Fluid Mech.* **509**, 145–179.

Qiu, L.-C. 2007 Numerical simulation of transient hydroelastic response of a floating beam induced by landing loads. *Appl. Ocean Res.* **29**, 91–98.

Qui, L.-C. & Liu, H. 2005 Transient hydroelastic response of VLFS by FEM with impedance boundary conditions in time domain. *China Ocean Engng* **19**, 1–9.

Squire, V. A. 2007 Of ocean waves and sea-ice revisited. *Cold Reg. Sci. Technol.* **49**, 110–133.

Stoker, J. J. 1957 *Water Waves: The Mathematical Theory with Applications*. Interscience.

Sturova, I. V. 2002*a* The action of periodic surface pressures on a floating elastic platform. *J. Appl. Math. Mech.* **66**, 71–81.

Sturova, I. V. 2002*b* Unsteady behaviour of an elastic beam floating on shallow water under external loading. *J. Appl. Mech. Tech. Phys.* **43**, 415–423.

Sturova, I. V. 2003 The action of an unsteady external load on a circular elastic plate floating on shallow water. *J. Appl. Math. Mech.* **67**, 407–416.

Sturova, I. V. 2006*a* The effect of periodic surface pressure on a rectangular elastic plate floating on shallow water. *J. Appl. Math. Mech.* **70**, 378–386.

Sturova, I. V. 2006*b* Unsteady behaviour of an elastic beam floating on the surface of an infinitely deep fluid. *J. Appl. Mech. Tech. Phys.* **47**, 71–78.

https://doi.org/10.1017/S0022112009990504 Published online by Cambridge University Press

Sturova, I. V. 2008*a* Effect of bottom topography on the unsteady behaviour of an elastic plate floating on shallow water. *J. Appl. Math. Mech.* **72**, 417–426.

Sturova, I. V. 2008*b* Unsteady behaviour of a heterogeneous elastic beam floating on shallow water. *J. Appl. Math. Mech.* **72**, 704–714.

Sturova, I. V. & Korobkin, A. A. 2005 Two-dimensional problem of periodic loading of an elastic plate floating on the surface of an infinitely deep fluid. *J. Appl. Mech. Tech. Phys.* **46**, 355–364.

Timoshenko, S. 1959 *Vibration Problems in Engineering,* 3rd ed. (In collaboration with D. H. Young), Van Nostrand.

Tkacheva, L. A. 2000 Eigenvibrations of a flexible platform floating on shallow water. *J. Appl. Mech. Tech. Phys.* **41**, 159–166.

Tkacheva, L. A. 2005*a* Action of a periodic load on an elastic floating plate. *Fluid Dyn.* **40**, 282–296.

Tkacheva, L. A. 2005*b* Vibrations of a floating elastic plate due to periodic displacements of a bottom segment. *J. Appl. Mech. Tech. Phys.* **46**, 754–765.

Watanabe, E. & Utsunomiya, T. 1996 Transient response analysis of a VLFS at airplane landing. In *Proceedings of the International Workshop on Very Large Floating Structures, Hayama, Japan,* November 1996, pp. 243–247.

Watanabe, E. & Utsunomiya, T. & Wang, C. M. 2004 Hydroelastic analysis of pontoon-type VLFS: a literature survey. *Engng Struct.* **26**, 245–256.

https://doi.org/10.1017/S0022112009990504 Published online by Cambridge University Press